Physica 7D (1983) 89–101
North-Holland Publishing Company

BIFURCATION AND CHAOS IN A PERIODICALLY STIMULATED CARDIAC OSCILLATOR

Leon GLASS, Michael R. GUEVARA and Alvin SHRIER
Department of Physiology, McGill University, 3655 Drummond Street, Montreal, Quebec, Canada H3G 1Y6

and

Rafael PEREZ
Instituto de Fisica, Universidad Nacional de Mexico, Mexico City, Mexico

Periodic stimulation of an aggregate of spontaneously beating cultured cardiac cells displays phase locking, period-doubling bifurcations and aperiodic "chaotic" dynamics at different values of the stimulation parameters. This behavior is analyzed by considering an experimentally determined one-dimensional Poincaré or first return map. A simplified version of the experimentally determined Poincaré map is proposed, and several features of the bifurcations of this map are described.

1. Introduction

Cardiac dysrhythmias are abnormal cardiac rhythms that often occur in diseased hearts. In what follows, we analyze biological and theoretical models for the generation of cardiac dysrhythmias that are associated with a lack of synchronization between autonomous pacemaker sites in the heart. The theoretical techniques are also applicable to a broader range of problems dealing with the synchronization of nonlinear oscillators to a periodic input.

In the normal human heart, the primary pacemaking site is located in the sinoatrial node (SAN). From the SAN the cardiac impulse spreads sequentially through the atrial musculature, the atrioventricular node (AVN), and specialized conducting tissues to the ventricles [1]. Electrical excitation of the atria is followed 0.08–0.12 sec later by excitation of the ventricles. The electrochemical events responsible for the spread of excitation can be monitored noninvasively by the electrocardiogram (ECG) which is a record of the potential differences between different points on the surface of the body. On the ECG, the P wave is associated with the excitation of the atria, the QRS complex with excitation of the ventricles, and the T wave with recovery of the excitability of the ventricles. Normally, excitation of cardiac tissue is associated with mechanical contraction. Fig. 1A shows a normal ECG. In a class of disorders called the atrioventricular (AV) heart blocks, there are abnormalities in the relative timing of the atrial and ventricular contractions. In first degree AV block the delay between the atrial and ventricular contractions is elevated above its normal maximal value. In second degree AV block, atrial contractions are not always followed by ventricular contractions. The second degree AV blocks are often periodic and are characterized by a ratio which gives the relative frequencies of atrial to ventricular contractions. Fig. 1B shows an example in which one cycle of 3:2 AV block (i.e. 3 atrial to 2 ventricular contractions) is followed by five cycles of 2:1 AV block. As well, second degree AV block can show extremely irregular or fluctuating rhythms (fig. 1C). In third degree AV block, there is an apparent lack of correlation between the atrial and ventricular rhythms, with separate pacemakers for each rhythm (fig. 1D). Finally, electro-

0167-2789/83/0000–0000/$03.00

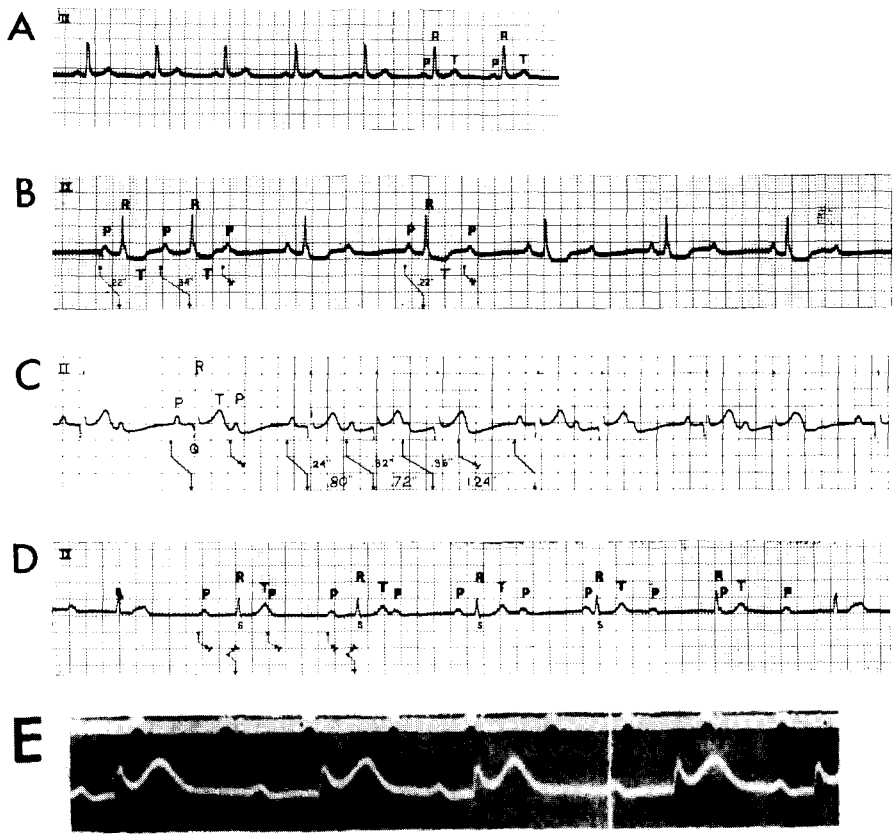

Fig. 1. Electrocardiograms illustrating normal and pathological cardiac rhythms. (A) Normal sinus rhythm. Each P wave is followed a fixed time later (the PR interval) by a QRS complex (1:1 ratio in atrioventricular conduction). (B) Second degree AV block with one 3:2 Wenckebach cycle followed by five consecutive 2:1 cycles. In the Wenckebach phenomenon, the PR interval following a dropped ventricular beat gradually increases until a P wave is not followed by a QRS complex (i.e. a ventricular beat is dropped). (C) Second degree AV block showing segments with 2:1, 4:3, and 3:2 conduction ratios. (D) Third degree heart block. Note the dissociation of the atrial and ventricular rhythms. (E) Sinus rhythm with alternating PR intervals (2:2 conduction). The laddergrams below the tracings of (B)–(D) schematically show the path of impulse formation and conduction. The small dots in these diagrams show sites of impulse generation, arrows show the spread of excitation, while short dark bars show regions of block of conduction. The sinoatrial node is at the top of the laddergram, the ventricles at the bottom. The time between the heavier vertical lines on the electrocardiographic paper is 0.20 sec, while the voltage difference between adjacent heavier horizontal lines is 0.5 mV. Time intervals in seconds are marked on some panels. (A)–(D) show human electrocardiograms reproduced with permission from [1], while (E) is from a cat reproduced with permission from [2].

cardiograms with alternating PR intervals (2:2 and 4:2 AV block) have been observed in animals [2] and in man [3, 4]. Fig. 1E shows an instance of 2:2 AV block published in 1910.

A fundamental hypothesis underlying our work is that changes in the cardiac rhythm can be associated with bifurcations in the qualitative dynamics of mathematical models describing generation and conduction of the cardiac impulse. The equations describing the electrical activity of the heart are complex and presumably vary from individual to individual. However, the qualitative features of the dynamics of these equations for the heart, and in particular their bifurcation structure, may well be similar in different individuals. Indeed, cardiac dysrhythmias have been classified by non-mathematicians (i.e. cardiologists) on the basis of their qualitative dynamics [1].

An early theoretical study of cardiac dysrhythmias was made by van der Pol and van der Mark in 1928 [5]. They showed that when three nonlinear oscillators (representing pacemaker sites of the heart) are coupled together, many different rhythms similar to the AV blocks can be observed as the relative frequencies and coupling parameters of the oscillators are varied. This pioneering work has since been extended by other researchers using analogue and digital models [6, 7]. As well, physiological studies have provided additional evidence that the canine heart contains a subsidiary pacemaker situated just below the AVN [8, 9]. However, most cardiac electrophysiologists ascribe the AV heart blocks to blocked conduction in the region of AVN [1], where there is assumed to be impulse conduction but no impulse generation. Mathematical models for this situation show correspondences with the AV heart blocks but do not show patterns with alternating PR intervals [10–12]. Our emphasis in the current work is on the effects of periodic stimulation of an autonomous cardiac oscillator. This situation may be applicable to the AV heart blocks, and also is relevant to a wide range of other situations, such as the artificial pacing of the heart and dysrhythmias such as parasystole.

Analysis of the effect of periodic forcing on relaxation oscillations of the van der Pol type have had a major impact on mathematics. Early studies demonstrated bistability (in which one of two different stable oscillating patterns is possible, depending on the initial conditions) as well as aperiodic dynamics [13, 14]. This observation of aperiodic dynamics in the 1940s played a role in the subsequent formulation of the horseshoe map by Smale (see the account in [15]). More recent studies of periodic forcing of nonlinear oscillators have shown that multistability and aperiodic dynamics can be accounted for by consideration of 1-dimensional maps of the circle into itself [16–18]. It has also been shown that such maps can display aperiodic dynamics that result from a cascade of period-doubling bifurcations [19–23].

Recent experimental studies on hydrodynamic [24–26], chemical [27, 28] and electronic [29–31] systems have shown the presence of complex dynamic behavior such as quasiperiodicity, period-doubling bifurcations, intermittency, and chaos. There is great interest in analyzing in detail the "universal" features of the transitions from periodic to chaotic dynamics [32–36].

In our research we have tried to develop biological models for cardiac dysrhythmias and to analyze experimentally observed dynamics. In section 2 we show that, under certain assumptions, the periodic stimulation of a cardiac oscillator by brief current pulses can be reduced to the analysis of a 1-dimensional map. In section 3 we consider the effects of periodic stimulation of spontaneously beating aggregates of cells obtained from embryonic chick heart [37]. In this work a current pulse generator is analogous to the SAN, whereas the heart cell aggregate is analogous to the subsidiary pacemaker located below the AVN. As the period of the stimulation changes, complex bifurcations including period-doubling bifurcations can be observed. In section 4 we investigate a 1-dimensional map that has been proposed as a simple model for periodic forcing of nonlinear oscillators. This map depends on 2 parameters corresponding to the strength and frequency of the periodic forcing.

2. Pulsatile stimulation of a cardiac oscillator: theory

In order to analyze the bifurcations of periodically stimulated cardiac oscillations mathematically, a number of assumptions are needed. In this section the main assumptions are explicitly stated. As well, the resulting properties of the dynamics are briefly discussed. Similar approaches have been previously employed [38–40]. More details on the mathematical aspects can be found in [41–43].

Assumption (*i*). A cardiac oscillator under normal conditions can be described by a system of ordi-

nary differential equations with a single unstable steady state and displaying an asymptotically stable limit cycle oscillation which is globally attracting except for a set of singular points of measure zero.

Assume the limit cycle has period T_0 and that we start with initial conditions $x(t=0)=x_0$, with x_0 being an arbitrary point on the limit cycle. Set the phase of x_0 to be zero. Then the phase of the point $x(t)$ is defined to be t/T_0 (mod 1). Thus, a phase $\phi (0 \leqslant \phi < 1)$ can be assigned to every point on the limit cycle. The eventual phase of points in the basin of attraction of the cycle can now be defined. Let $x(t=0)$ and $x'(t=0)$ be the initial conditions of a point on the cycle and a point not on the cycle respectively, and $x(t)$, $x'(t)$, be the coordinates of the trajectories at time t. If $\lim_{t\to\infty} d(x(t), x'(t)) = 0$, where d is the Euclidean distance, then the eventual phase of $x'(t=0)$ is the same as the phase of $x(t=0)$. A locus of points all with the same eventual phase is called an isochron. If the equations describing the system are of dimension 2, then there must be at least one singular point at which the eventual phase is not defined (fig. 2). If the system of equations is of order greater than 2, then there must exist a set of dimension $\geqslant 1$ consisting of points where the eventual phase is not defined [41–43].

Consider the effect of delivering a stimulus starting at a time when the oscillator is at some (old) phase ϕ $(0 \leqslant \phi < 1)$. In general, at the end of the perturbation, the orbit will lie on a different isochron of (new) phase θ. Then

$$\theta = g(\phi), \tag{1}$$

where the function g depends on the stimulus amplitude and duration. The function g is often called the phase transition curve (PTC) [42]. Note that there can also be a stimulus which will perturb the oscillator to a phaseless point.

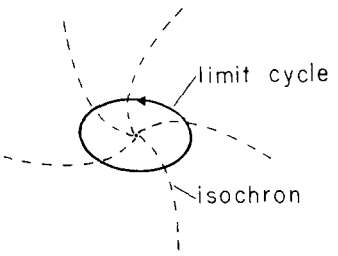

Fig. 2. Phase space of a 2-dimensional nonlinear oscillator. The solid oriented closed curve is the limit cycle, while the dashed curves represent isochrons. The point in the center is an equilibrium point, and therefore is phaseless and does not lie on any isochron.

Assumption (ii). Following a short perturbation, the time course of the return to the limit cycle is much shorter than the spontaneous period of oscillation or the time between periodic pulses.

This assumption allows one to measure the PTC for the cardiac preparation and use the experimentally measured PTC to compute the effects of periodic stimulation. Assume that one of the variables in the system is experimentally measurable. Define a reference or marker event to be a particular point on the waveform (e.g. the maximum value attained). The time between two consecutive marker events of the spontaneous cycle is the period T_0 of the oscillation. Fig. 3A shows the situation schematically. A stimulus (which we assume is a delta function) is delivered at a time δ following the preceding spontaneous event. The duration T of the perturbed cycle is the time from the event preceding the stimulus to the event immediately subsequent to the stimulus. Note that due to fast relaxation back to the limit cycle, the post-stimulus cycles are approximately of duration T_0. Thus, essentially all of the eventual phase shift occurs within the perturbed cycle. Therefore

$$T/T_0 = 1 + \phi - \theta, \tag{2}$$

where $\phi = \delta/T_0$ (fig. 3B). Since T can be experimentally measured for a given ϕ, and T_0 is known, the PTC can be determined (fig. 3C).

Now consider the effects of periodic stimulation with a time τ between successive stimuli. Calling ϕ_i (mod 1) the phase of the oscillator immediately before the ith stimulus we obtain

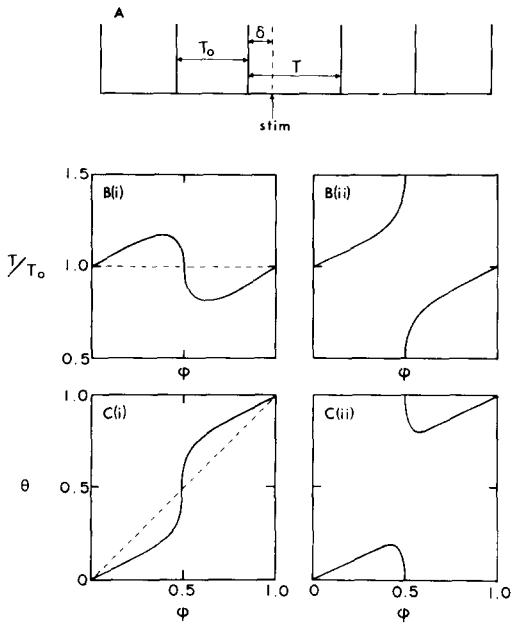

Fig. 3. (A) Schematic diagrams illustrating the effect of perturbation of a limit cycle oscillator by a single impulse. The vertical lines represent the occurrence of a marker event (see text). The spontaneous time between marker events (the period of the limit cycle) is denoted by T_0. A stimulus is delivered at a time δ after a marker event, causing a change in the cycle length from T_0 to T. The durations of the cycles following the perturbed cycle are all very close to T_0. (B) The normalized perturbed interbeat interval T/T_0 plotted as a function of the old phase $\phi = \delta/T_0$. (C) The new phase-old phase curve (phase transition curve or PTC) computed from (B) using eq. (2). In part (i) of (B) and (C), the stimulus is weak enough to produce type 1 phase resetting, while in (ii) it is sufficiently strong to result in type 0 behavior. The curves of (B) and (C) are taken from a very simple limit cycle model [19].

$$\phi_{i+1} = f(\phi_i) = g(\phi_i) + \tau/T_0, \tag{3}$$

where $g(\phi)$ is the experimentally determined PTC for that stimulus strength and $g(\phi + j) = g(\phi) + j$ for j an integer. Eq. (3) represents a first return or Poincaré map. Starting from an initial phase ϕ_0, one can iterate eq. (3) to generate a sequence ϕ_0, $\phi_1 = f(\phi_0), \ldots, \phi_N = f(\phi_{N-1}) = f^N(\phi_0)$. If

$$\begin{aligned} &\phi_N^* (\text{mod } 1) = \phi_0^* (\text{mod } 1), \\ &\phi_i^* (\text{mod } 1) \neq \phi_0^* (\text{mod } 1), \quad 1 \leqslant i < N, \end{aligned} \tag{4}$$

then ϕ_0^* is said to be a fixed point of period N and $\phi_0^*, \phi_1^*, \ldots, \phi_{N-1}^*$ is a cycle of period N. The cycle is stable if

$$\left| \left(\frac{\partial f^N}{\partial \phi_i} \right)_{\phi_i = \phi_0^*} \right| = \prod_{j=0}^{N-1} \left| \left(\frac{\partial f}{\partial \phi_i} \right)_{\phi_i = \phi_j^*} \right| < 1. \tag{5}$$

If an extremum of the function f is a point on a cycle, the slope computed from eq. (5) equals zero, and the cycle is called a superstable cycle. A stable cycle of period N corresponds to stable $N:M$ phase locking with

$$M = \sum_{i=1}^{N} [g(\phi_i^*) - \phi_i^* + \tau/T_0]. \tag{6}$$

The rotation number is defined as

$$\rho = \lim_{i \to \infty} \frac{\phi_i - \phi_0}{i}. \tag{7}$$

For stable $N:M$ phase locking the rotation number is rational, $\rho = M/N$. In section 3 we use eq. (3) to predict the properties of the periodically stimulated cardiac preparation. The observation of good agreement between the theoretical predictions and experimental observations provides a posteriori justification for assumption (ii). However, a careful experimental and theoretical analysis of the consequences of the breakdown of assumption (ii) has not yet been performed.

Assumption (iii). The topological characteristics of the PTC change in stereotyped ways as the stimulus strength increases.

As a consequence of assumption (i) the PTC is a continuous map of the unit circle into itself $g: S^1 \to S^1$. The topological degree (or winding number) of g is the number of times θ traverses the unit circle as ϕ traverses the unit circle once. At zero perturbation strength $\theta = \phi$ so that by continuity the PTC is a monotonic map of degree 1 for sufficiently small perturbation (fig. 3C(i)). As the stimulus strength increases from zero, our experimental studies seem to indicate that the PTC

remains of degree 1, but undergoes a transition from a monotonic to a non-monotonic function. Winfree [43] has given evidence that at high stimulus strength the PTCs for neural and cardiac oscillators can be of degree zero and therefore non-monotonic (fig. 3C(ii)). We conjecture that as stimulus strength increases the PTC for biological oscillators will, provided assumption (i) is satisfied, in general undergo the sequence of transitions

degree 1 (monotonic)→degree 1 (nonmonotonic)→degree 0.

We have previously considered the case of a model oscillator in which, as the stimulus strength is increased, the PTC undergoes a direct transition from degree 1 (monotonic) to degree 0 [19]. In section 4 we consider the properties of a simple model of phase locking in which the PTC undergoes a transition from degree 1 (monotonic) to degree 1 (non-monotonic).

3. Pulsatile stimulation of a cardiac oscillator: experiment [37]

As an application of the theory presented in section 2, we consider the effects of single and periodic stimulation of spontaneously beating aggregates of cells taken from the ventricles of 7-day-old embryonic chick heart. Spheroidal aggregates (100–200 μm in diameter) of electrically coupled cells were maintained in tissue culture [44, 45]. Each aggregate beats spontaneously with a period between 0.4 and 1.3 sec. Cells within a single aggregate are very nearly isopotential [46]. The voltage difference across the cell membrane is measured using a glass microelectrode filled with KCl, inserted into one cell of a beating aggregate. Current pulses are delivered through the same microelectrode.

In Fig. 4 are shown the effects of brief injection of current at different phases ($\phi = \delta/T_0$) of the cardiac cycle (for two different current strengths). Note that at the higher current strength there is a very rapid change in the perturbed interbeat interval T for stimuli delivered at times from 150 ms to 170 ms into the cycle. One expects, based on theoretical considerations that the plot of T versus ϕ can be discontinuous for sufficiently high current strengths [42]. From experiments, it is difficult (and perhaps impossible) to establish whether such curves are indeed discontinuous.

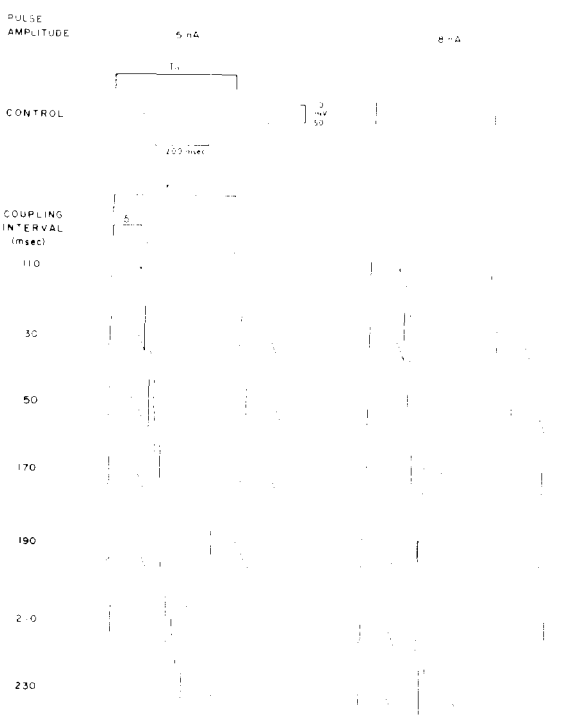

Fig. 4. Transmembrane voltage recorded from an aggregate. The uppermost tracings each show one cycle of spontaneous activity. The left and right panels show the effects of delivering 5 nA and 8 nA constant current pulses (20 msec duration) at different coupling intervals. The coupling interval δ is the time to the beginning of the stimulus from the upstroke of the immediately preceding action potential. The perturbed interbeat interval is denoted by T. Note that as the stimulus intensity is increased from 5 nA to 8 nA, the transition from prolongation to shortening of the perturbed cycle becomes more abrupt and occurs at a shorter coupling interval. The interbeat interval of the cycle following the perturbed cycle is almost equal to the control interbeat interval in the three traces of the right-hand panel that show such cycles.

Using the T/T_0 data obtained from the single pulse perturbation experiments (fig. 5C) and eq. (2), it is possible to construct the return map given

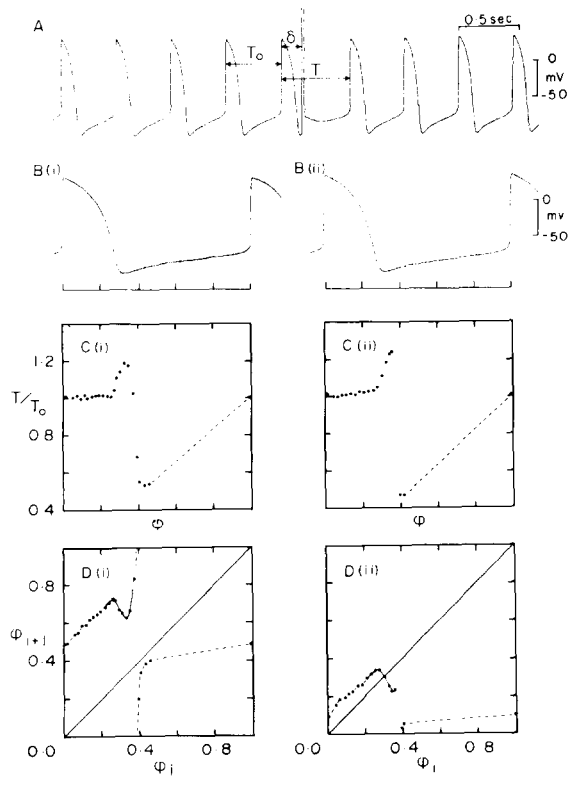

Fig. 5. (A) Transmembrane potential from an aggregate as a function of time, showing spontaneous electrical activity and the effect of a 20 msec, 9 nA depolarizing pulse delivered at an interval of 160 msec following the action potential upstroke. In (B to D), parts (ii) show results from this aggregate (aggregate 2), while parts (i) are from aggregate 1, taken from a different culture. (B) Membrane voltage as a function of phase ϕ, $0 \leqslant \phi < 1$. (C) Phase-resetting data, showing the normalized length T/T_0 of the perturbed cycle as a function of ϕ. (i) Pulse duration 40 msec, pulse amplitude 5 nA; (ii) pulse duration 20 msec, pulse amplitude 9 nA. For approximately $0.4 < \phi < 1.0$ the action potential upstroke occurs during the stimulus artifact and hence the perturbed cycle length cannot be exactly determined. The dashed line represents a linear interpolation that approximates the data. During collection of these data, the average control interbeat intervals (± 1 standard deviation) were (i) $\Gamma_0 = 515 \pm 5.7$ msec and (ii) $\Gamma_0 = 434 \pm 5.5$ msec. (D) Poincaré maps computed from eq. (3) and the data in fig. 5C; (i) $\tau = 250$ msec, (ii) $\tau = 480$ msec. The dashed line represents a linear interpolation used in iterating the Poincaré map; the solid line through the data points is a quartic fit for $0.22 < \phi_i < 0.37$. Reprinted from [37] with permission.

by eq. (3). Examples of return maps from two different aggregates are shown in fig. 5D. Using eqs. (3)–(5), the experimentally derived return maps can be iterated to compute the response to periodic stimulation. The numerically predicted phase locking regions (fig. 6B) are compared with experimental observations (fig. 6A). In fig. 6C are shown the stable phases in the period-doubling zone.

Representative traces of microelectrode recordings at different stimulation frequencies are shown in fig. 7. Regular and irregular dynamics theoretically predicted in fig. 6 were observed. Notice that in fig. 7C(i) (aggregate 1) there is a spontaneous change from 1:1 to 2:2 phase locking at a stimulation period of 550 ms. Stimulation of the second aggregate at a period of 490 ms produced both 4:4 and irregular patterns (fig. 7C(ii) and fig. 7C(iii) respectively). Computations show that 2:2 and 4:4 phase-locking as well as chaotic dynamics are predicted in the range 460–490 ms for this aggregate (fig. 6C).

There are several reasons to expect discrepancies between the theoretically predicted and experimentally observed dynamics. First, assumption (ii) in section 2 is not strictly satisfied since there can be slight changes in the rate of the preparation for several beats following the injection of a single stimulus. The following two additional physiological considerations are also important:

i) *There is biological "noise" intrinsic to the experimental preparation as well as environmental "noise" which is not accounted for in the theory.* Although the fluctuations in interbeat interval in the absence of stimulation are comparatively small, some of the experimentally observed irregular patterns may not be due to intrinsic aperiodicity in the dynamical system itself, but rather to the effects of biological "noise" generated within the preparation or environmental "noise" arising from fluctuating ambient conditions. In addition, some of the irregularity in deterministically aperiodic patterns (such as that shown in fig. 7C (iii) which is ascribed to "chaotic" dynamics arising out of a cascade of period-doubling bifurcations) may well be accounted for by "noise". Additional analysis is needed to determine the effect of "noise" on

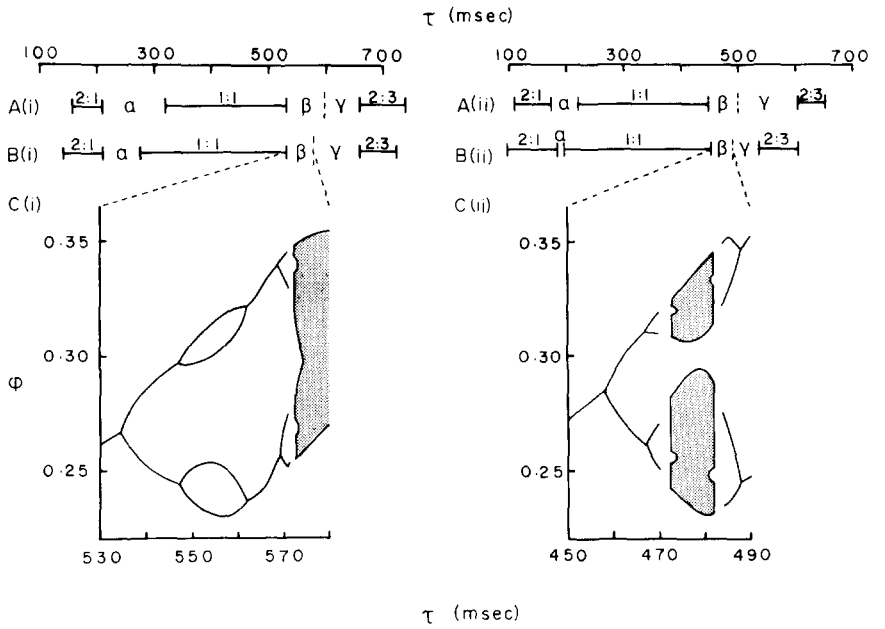

Fig. 6. Experimentally determined and theoretically computed responses to periodic stimulation of period τ with the same pulse durations and amplitudes as in fig. 5C. Parts (i) refer to aggregate 1, parts (ii) to aggregate 2. (A) Experimentally determined dynamics: there are three major phase-locking regions (2:1, 1:1, 2:3) and three zones of complicated dynamics labelled α, β and γ. (B) Theoretically predicted dynamics; note agreement with (A). (C) Theoretically predicted dynamics in zone β: curves give phase or phases in the cycle at which the stimuli fall during 1:1, 2:2 and 4:4 locking; stippled regions show the range of phases in which the stimulus falls during irregular dynamics. Reprinted from [37] with permission.

"chaos" and thus to determine the extent to which "noise" is implicated in generating the irregular dynamics experimentally observed.

ii) *Prolonged periodic stimulation of the aggregate changes the properties of the aggregate.* Following a long period of periodic stimulation with 1:1 synchronization at frequencies higher than the intrinsic aggregate beating frequency, the cessation of stimulation leads to a transient slowing of the beat rate below the control value ("overdrive suppression"). Conversely, after a period of "underdrive", "underdrive acceleration" occurs during the post stimulation recovery period [47]. The spontaneous transition from 1:1 to 2:2 phase locking observed in fig. 7C(i) during stimulation at a fixed frequency could arise from an increase in the intrinsic frequency of the aggregate secondary to underdrive.

Despite these considerations, there is good agreement between theory and experiment. However, probably as a consequence of "noise", we have not been able to observe phase locking patterns which are theoretically computed to extend over small regions of parameter space [48–50]. Consequently, experimental observation of the Feigenbaum constant, such as has been performed in periodically forced electronic oscillators [30, 31] and in experiments on turbulence [25] will be exceedingly difficult in this and other biological preparations. On the other hand, biological preparations may be ideal systems to analyze the effects of "noise" in systems which would be predicted to be deterministically "chaotic" in the absence of noise [51].

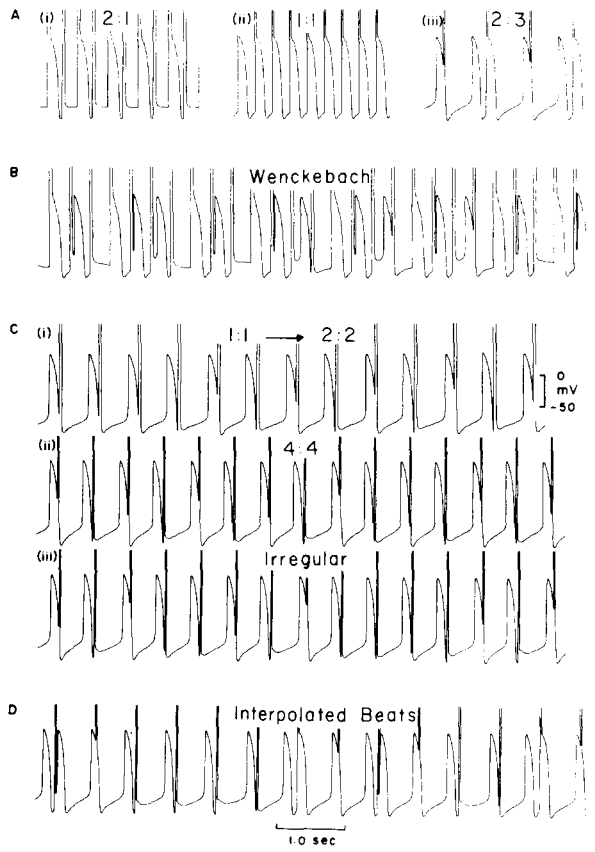

Fig. 7. Representive transmembrane recordings from both aggregates showing the effects of periodic stimulation with the same pulse durations and amplitudes as in fig. 5C. (A) Stable phase-locked patterns: (i) 2:1 (aggregate 1, $\tau = 210$ ms); (ii) 1:1 (aggregate 2, $\tau = 240$ ms); (iii) 2:3 (aggregate 2, $\tau = 600$ ms). (B) Dynamics in zone α: irregular dynamics displaying the Wenckebach phenomenon (aggregate 1, $\tau = 280$ ms). (C) Dynamics in zone β: (i) 1:1 phase locking spontaneously changing to 2:2 phase locking (aggregate 1, $\tau = 550$ ms). During 2:2 phase locking there are two distinct phases of the cycle at which the stimuli fall. (ii) 4:4 phase locking (aggregate, 2, $\tau = 490$ ms). There are four distinct phases of the cycle at which the stimuli fall. (iii) Irregular dynamics with one action potential in each stimulus cycle (aggregate 2, $\tau = 490$ ms). There is a narrow range of phases in which the stimuli fall. (D) Dynamics in zone γ: irregular dynamics displaying escape or interpolated beats (aggregate 2, $\tau = 560$ ms). Reprinted from [37] with permission.

4. A model map [22, 23]

Numerical computation of phase locking using the experimentally determined Poincaré map has shown complex bifurcations. In this section we discuss the possibility that a large topological class of maps might display the same bifurcation structure as the experimentally determined maps. Such behavior may be anticipated since the bifurcations for the one parameter map of the interval into itself with a single maximum are largely independent of the functional form of the map [32, 33].

Consider the map given in eq. (3) where $g(\phi)$ is a continuous function defined on the real line and $\deg[g(\phi) \pmod 1] = 1$. Assume there is a single maximum at ϕ_{max} and a single minimum at ϕ_{min} in the interval [0, 1] (fig. 5D(i)). Let $\phi_i = H_i(\tau)$ where the $H_i(\tau)$ are functions found by iterating eq. (3) from $\phi_0 = \phi_{max}$. For j an integer, $g(x+j) = g(x)+j$, and

$$H_N(j) - H_N(j-1) = N. \tag{8}$$

There will be a superstable cycle for each value of τ for which $\phi_0 \pmod 1 = H_N(\tau) \pmod 1$. Since $H_N(\tau) \pmod 1$ equals any fixed value between 0 and 1 at least N times as τ varies from $j-1$ to j, there will be a minimum of N superstable cycles associated with N different rotation numbers occurring at N distinct values of τ. The iterates of the minimum also give rise to superstable cycles. Consequently, *there will be at least two values of τ at which there exist superstable cycles for each rational rotation number* [22]. This fixed point theorem does not depend on the functional form of g.

The 1-dimensional, two parameter map

$$\phi_{i+1} = f(\phi_i) = \phi_i + b \sin 2\pi\phi_i + \tau, \tag{9}$$

where b is a real number has recently been discussed by several workers as a model for periodically forced nonlinear oscillators [22, 23, 35, 36, 40]. For $b < 1/2\pi$, $f(\phi_i)$ is a monotonic function and it is known from early studies that the rotation number is a monotonic function of τ and that only periodic and quasiperiodic dynamics exist [52]. In addition, recent studies have described the application of renormalization methods to analyze the dynamics for $0 < b \leqslant 1/2\pi$ [35, 36]. We primarily

consider the dynamics for $b > 1/2\pi$ [20–23]. In this region $f(\phi_i)$ is not monotonic.

For eq. (9) it is straightforward to show that there exists a stable fixed point of period 1 at

$$\phi^* = \frac{1}{2\pi} \sin^{-1}\left(\frac{1-\tau}{b}\right) \tag{10}$$

(corresponding to 1:1 phase locking) for

$$(1-\tau)^2 < b^2 < (1-\tau)^2 + \pi^{-2}. \tag{11}$$

The stable period 1 orbit appears via a tangent bifurcation $(\partial f/\partial\phi)_{\phi^*} = 1$ at $b = 1-\tau$ and loses its stability via a period-doubling bifurcation $(\partial f/\partial\phi)_{\phi^*} = -1$ at $b = |(1-\tau)^2 + \pi^{-2}|^{1/2}$. In addition, for $\tau = 1$ it is easy to compute that there is a further bifurcation to two stable period 2 orbits with rotation number 1 (2:2 phase locking) at $b = 0.5$ and a bifurcation to two stable period 4 orbits (4:4 phase locking) at $b = (0.25 + 1/2\pi^2)^{1/2}$. For $\tau = 1.5$ there is a period-doubling bifurcation from a period 2 cycle (2:3 phase locking) to a period 4 cycle (4:6 phase locking) at $b = \pi^{-1}2^{-1/2}$.

Further results on the boundaries of the phase locking zones were obtained by numerical analysis. The Poincaré map in eq. (9) was numerically iterated from different ϕ_0 at many points in the (b, τ) parameter space. The results are shown in fig. 8. For many regions in the parameter space there is bistability in that one of two stable cycles is asymptotically reached depending on the initial condition ϕ_0. In addition, evidence for chaotic dynamics (a positive Lyapunov number) was found [23].

The 1:1 phase locking region arises by a tangent bifurcation along one boundary and is lost via a period doubling bifurcation along the other boundary. Consequently, since the slope of the period 1 cycle is a continuous function of b and τ, there must be a locus of points with period 1 along which the slope is equal to zero. Along the locus, the maximum (or minimum) of the Poincaré map will be on the cycle and the cycle is called a superstable cycle. This will occur for

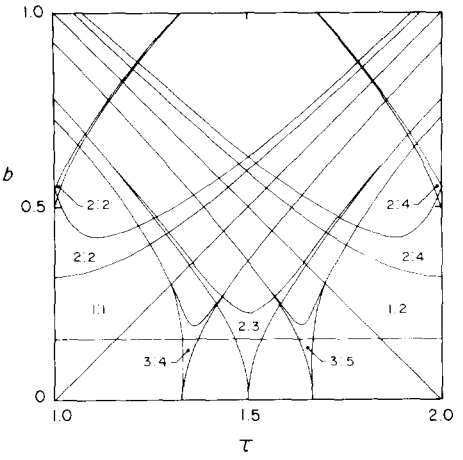

Fig. 8. Locally stable phase locking regions for eq. (9). The line at $b = 1/2\pi$ separates the regions in which eq. (9) is a monotonic function on the unit circle ($b < 1/2\pi$) and a nonmonotonic function ($b > 1/2\pi$). The widths of some of the phase locking zones (e.g. 3:4, 2:3) become so narrow as b increases that the boundaries have been collapsed into a single line in the drafting of the figure. In the non-labelled regions are phase-locked, quasiperiodic and chaotic dynamics. Slightly modified from [23] with permission.

$$(1-\tau)^2 + 1/4\pi^2 = b^2, \tag{12}$$

where for $\tau < 1$ the points defined by eq. (12) are derived from the maximum and for $\tau > 1$ the points defined by eq. (12) are derived from the minimum.

The loci of the superstable cycles are called the skeleton [22]. In fig. 9 are shown the boundaries of the $N:M$ phase locking zones ($1 \leqslant N \leqslant 5$) for $0 < b < 1/2\pi$ and the associated skeleton for $b > 1/2\pi$. Fig. 10 shows the skeleton derived from the maximum $\phi_{\max}$ for $N \leqslant 3$.

A branch of the skeleton extending downwards to $b = 1/2\pi$ is called a primary branch, and all other branches are called secondary. (This terminology is due to S. Shenker who has independently observed the following properties). Since no two branches of the skeleton derived from the maximum can intersect, and the skeleton of the 1:1 phase locking asymptotically approaches the line $b = 1-\tau$ the slope of all branches of the skeleton derived from the maximum must be asymptotically

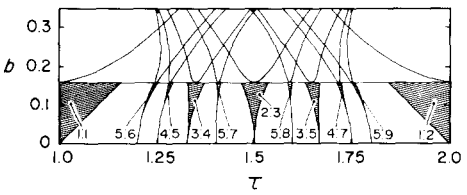

Fig. 9. The $N:M$ phase locking regions for $1 \leqslant N \leqslant 5$ for $b < 1/2\pi$ and the associated superstable cycles for $b > 1/2\pi$ for eq. (9). From [22] with permission.

equal to -1 for sufficiently large values of b. Further, all primary branches derived from the maximum must maintain the ordering given by monotonically increasing rotation numbers for fixed b as τ increases (fig. 10). Finally, in fig. 11, we show the skeleton of the phase locking zones up to period 4 with $\rho = 1$. Limited numerical analysis indicates a topologically equivalent skeleton appears in other V-shaped regions formed by the primary branches of the skeleton for each rational rotation number.

On the basis of these numerical and analytical results we have proposed the following structure for the skeleton and phase locking zones of eq. (9) [22]. Each zone of stable phase locking for $b < 1/2\pi$ extends through $b = 1/2\pi$ and then splits into two branches (figs. 8 and 9). In the V-shaped region of the extensions of each "Arnold tongue"

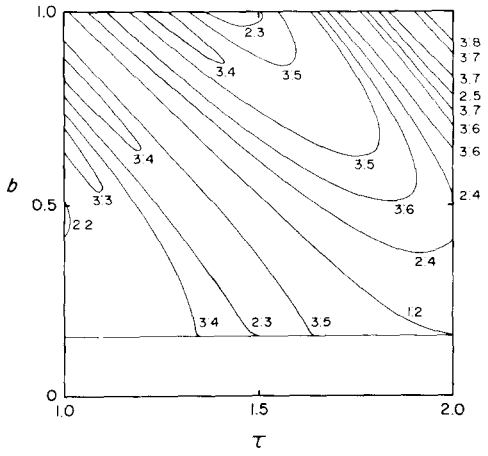

Fig. 10. The period N superstable cycles for $1 \leqslant N \leqslant 3$ derived from ϕ_{max} for eq. (9). There is a symmetrically located set of superstable cycles found from iteration of ϕ_{min}.

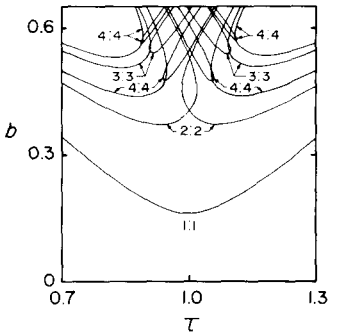

Fig. 11. Superstable cycles associated with $N:N$ phase locking patterns, $1 \leqslant N \leqslant 4$ (rotation number $\rho = 1$). From [22] with permission.

are period-doubling bifurcations. The skeleton of the phase locking zones in each one of these V-shaped regions is topologically equivalent to the skeleton for $\rho = 1$ (fig. 11), but with a different rotation number.

There is considerable interest in the transition from quasiperiodic to chaotic dynamics in physical systems and mathematical models [35, 36, 53]. In the current context one question is, "What happens to the quasiperiodic orbits (i.e. those with irrational rotation number) known to exist when $b < 1/2\pi$ as b passes through the value $b = 1/2\pi$?" For a map of the circle into itself, for a set of parameters for which there is bistability with two different rotation numbers, there will be initial conditions which give all intermediate rotation numbers [17]. A consequence of the bistability of the sine map for $b > 1/2\pi$ is that for $b > 1/2\pi$ orbits with a given irrational rotation number will be present in a wedge shaped region whose tip is on the line $b = 1/2\pi$. It should be possible to describe the aperiodic orbits associated with an irrational rotation number using techniques developed in symbolic dynamics and kneading theory [16, 17]. However, if there is bistability it is still not known if almost all points will attract to one of the two stable periodic orbits. Finally, this discussion has been concerned with analysis of 1-dimensional maps. A careful analysis of the breakdown of quasiperiodic dynamics in 2-dimensional maps has shown an overlapping of Arnold tongues similar to that shown in figs. 8 and 9 [53].

5. Conclusions

We have shown that the effects of periodic pulsatile stimulation of a cardiac oscillator can be analyzed by consideration of a 1-dimensional map which is obtained from experimental measurements. The dynamics in response to periodic stimulation are predicted by iterating this experimentally derived map and bear a close correspondence to the experimentally observed dynamics. In particular, stable phase locking, period-doubling bifurcations and aperiodic dynamics are all theoretically computed and experimentally observed. The experimentally observed dynamics show patterns similar to many commonly observed cardiac dysrhythmias. Furthermore, this work gives a novel perspective to some of the aperiodic cardiac dynamics clinically observed as well as uncommon phase locked rhythms such as 2:2 and 4:2 AV block. We have also analyzed the dynamics for a simple Poincaré map (the sine map in eq. (9)) and discussed period-doubling bifurcations, bistability and chaos in this model system.

Experimentally observed transitions from periodic to chaotic dynamics in physical systems can often be accounted for, at least qualitatively, by the bifurcations in simple 1- and 2-dimensional maps under parametric changes [26–29]. Unfortunately, in this work, it is not yet possible to compute from first principles the underlying maps which give a phenomenological correspondence with theory. Consequently, the study of periodic forcing of oscillations by short pulsatile inputs has advantages over other experimental techniques and may be useful in other physical systems. There are many similarities between the experimentally measured 1-dimensional map for the cardiac oscillator and the maps derived from other experimental systems [26–29]. Clearly, further work is needed to carefully probe experimentally observed dynamics in physical and biological systems and to clarify the bifurcation structure of maps which display quasi-periodic, periodic and aperiodic dynamics.

Analysis of the mathematics describing cardiac dysrhythmias has potentially rich rewards in the diagnosis and treatment of heart disease. We hope that our work will help stimulate interest in these problems by mathematicians and physicists.

Acknowledgments

This research has been supported by grants from the Natural Sciences and Engineering Research Council of Canada and the Canadian Heart Foundation. MRG is a recipient of a predoctoral traineeship from the Canadian Heart Foundation. We thank John Guckenheimer, James Sethna and Scott Shenker for helpful conversations. The manuscript was partially written while LG was in residence at the Aspen Center for Physics.

References

[1] S. Mangiola and M.C. Riota, Cardiac Arrhythmias: Practical ECG Interpretation, 2nd Edition (J.B. Lippincott, Philadelphia, 1982).
[2] T. Lewis and G.C. Mathison, Heart 2 (1910) 47.
[3] M. Segers, Arch. Mal. Coeur 44 (1951) 525.
[4] R. Langendorff, Am. Heart J. 55 (1958) 181.
[5] B. van der Pol and J. van der Mark, Phil. Mag. 6 (1928) 763.
[6] D.A. Sideris and S.D. Moulopoulos, J. Electrocardiol. 10 (1977) 51.
[7] C.R. Katholi, F. Urthaler, J. Macy Jr. and T.N. James, Comp. Biomed. Res. 10 (1977) 529.
[8] F.A. Roberge, R.A. Nadeau and T.N. James, Cardiovasc. Res. 2 (1968) 19.
[9] T.N. James, J.H. Isobe and F. Urthaler, Circ. Res. 45 (1979) 108.
[10] M.B. Berklinblit, in I.M. Gelfand, V.S. Garfinkel, S.V. Fomin and M.L. Tsetlin (eds.), Models of the Structural -Functional Organization of Certain Biological Systems (MIT Press, Cambridge, 1971) p. 155.
[11] H.D. Landahl and D. Griffeath, Bull. Math. Biophys. 33 (1971) 27.
[12] J.P. Keener, J. Math. Biol. 12 (1981) 589.
[13] M.L. Cartwright and J.E. Littlewood, J. Lond. Math. Soc. 20 (1945) 180.
[14] N. Levinson, Ann. of Math. 50 (1949) 127.
[15] S. Smale, The Mathematics of Time (Springer, New York, 1980) p. 147.
[16] M. Levi, Memoirs Amer. Math. Soc. 32, Number 244 (1981).
[17] J. Guckenheimer, in Dynamical Systems (Birkhauser, Boston, 1980) p. 115.

[18] P. Coullet, C. Tresser and A. Arneodo, Phys. Lett. 77A (1980) 327.
[19] M.R. Guevara and L. Glass, J. Math. Biol. 14 (1982) 1.
[20] T. Geisel and J. Nierwetberg, Phys. Rev. Lett. 48 (1982) 7.
[21] M. Schell, S. Fraser and R. Kapral, Phys. Rev. A 26 (1982) 504.
[22] L. Glass and R. Perez, Phys. Rev. Lett. 48 (1982) 1772.
[23] R. Perez and L. Glass, Phys. Lett. 90A (1982) 441.
[24] P.R. Fenstermacher, H.L. Swinney, S.V. Benson and J.P. Gollub, Ann. N.Y. Acad. Sci. 316 (1979) 652.
[25] A. Libchaber, C. Laroche and S. Fauve, J. Physique Lett. 43 (1982) L-211.
[26] A. Arneodo, P. Coullet, C. Tresser, A. Libchaber, J. Maurer and D. d'Humières, in press (1982).
[27] A.S. Pikovsky, Phys. Lett. 85A (1981) 13.
[28] R. Simoyi, A. Wolf and H. Swinney, Phys. Rev. Lett. 49 (1982) 245.
[29] J.P. Gollub, E.J. Romer and J.E. Socolar, J. Stat. Phys. 23 (1980) 321.
[30] P.S. Linsay, Phys. Rev. Lett. 47 (1981) 714.
[31] J. Testa, J. Perez and C. Jeffries, Phys. Rev. Lett. 48 (1982) 714.
[32] R.M. May, Nature (London) 261 (1976) 459.
[33] M.J. Feigenbaum, J. Stat. Phys. 19 (1978) 25.
[34] J.-P. Eckmann, Rev. Mod. Phys. 53 (1981) 643.
[35] D. Rand, S. Ostlund, J. Sethna and E.D. Siggia, Phys. Rev. Lett. 49 (1982) 132.
[36] M.J. Feigenbaum, L. P. Kadanoff and S.J. Shenker, in press (1982).
[37] M.R. Guevara, L. Glass and A. Shrier, Science 214 (1981) 1350.
[38] D.H. Perkel, J.H. Schulman, T.H. Bullock, G.P. Moore and J.P. Segundo, Science 145 (1964) 61.
[39] S.W. Scott, Ph.D. Thesis, S.U.N.Y. (Buffalo), (1979).
[40] G.M. Zaslavsky, Phys. Lett. 69A (1978) 145.
[41] M. Kawato and R. Suzuki, Biol. Cybernetics 30 (1978) 241.
[42] M. Kawato, J. Math. Biol. 12 (1981) 13.
[43] A.T. Winfree, The Geometry of Biological Time (Springer, New York, 1980).
[44] R.L. DeHaan, Dev. Biol. 23 (1970) 226.
[45] R.L. DeHaan and L.J. DeFelice, Theor. Chem. 4 (1978) 181.
[46] L.J. DeFelice and R.L. DeHaan, Proc. IEEE 65 (1977) 796.
[47] D.L. Ypey, W.P.M. VanMeerwijk and R.L. DeHaan, in L.N. Bouman and H.J. Jongsma (eds.), Cardiac Rate and Rhythm (Martinus Nijhoff, The Hague, 1982) p. 363.
[48] J.P. Crutchfield and B.A. Huberman, Phys. Lett. A77 (1980) 407.
[49] L. Glass, C. Graves, G.A. Petrillo and M.C. Mackey, J. theor. Biol. 86 (1980) 455.
[50] R. Guttman, L. Feldman and E. Jakobsson, J. Membr. Biol. 56 (1980) 9.
[51] J. Guckenheimer, Nature 298 (1982) 358. See also J. Crutchfield and N. Packard, this volume.
[52] V.I. Arnold, Translations A.M.S. 2nd Series, 46 (1965) 213.
[53] D.G. Aronson, M.A. Chory, G.R. Hall and R.P. McGehee, Commun. Math. Phys. 83 (1982) 303.